International Journal of Concrete Structures and Materials

RESEARCH

Prediction of the Tensile Strength of Normal and Steel Fiber Reinforced Concrete Exposed to High Temperatures

Mehrdad Abdi Moghadam[1*] and Ramezan Ali Izadifard[2]

Abstract

The tensile strength of concrete has a great impact on the performance of concrete structures, especially for members exposed to high temperatures. The inclusion of steel fibers in concrete is one of the measures to retrieve the loss of tensile strength. The previous equations for the prediction of the tensile strength, are valid for conventional concrete and can predict the tensile strength after high-temperature exposure. Therefore, they are unsatisfactory for forecasting the tensile strength of plain and steel fiber reinforced concrete under high-temperature exposure. To establish a model that can effectively simulate the tensile strength of plain concrete, specimens with compressive strengths of 20–80 MPa are tested. Then by performing tensile strength tests on the specimens containing various content of steel fiber, an equation for prediction of the tensile strength at the ambient temperature is proposed. Meanwhile, the tensile strength tests are conducted at temperatures of 100–800 °C to develop a model for high-temperature exposure. The results indicate that an increase of compressive strength from 20 to 84 improves the tensile strength by 169.4%, and the incorporation of 0.25 and 0.5% of steel fibers can improve the tensile strength of normal concrete by 58.48 and 80.29% on average at the tested temperatures, respectively. Moreover, the proposed model is able to predict the tensile strength of normal and steel fiber reinforced concrete exposed to high temperatures accurately. This equation would help a wider application of the steel fibers in the construction industry with the risk of a fire accident.

Keywords: Tensile strength, Strength prediction, Fiber content, High temperature, Steel fiber, Regression Analysis

1 Introduction

One of the widely used construction materials is concrete which enjoys a higher compressive strength in comparison with tensile strength. The relatively low tensile strength of concrete breeds a weak resistance to crack propagation. Propagation of cracks damages the concrete members, which is intensified for members exposed to high temperatures. Concrete may be exposed to high temperatures such as the chimneys, the furnaces, the runway of airports, factories where

melting of metals occur, and structures with the risk of fire. High temperatures can induce a severe physical and chemical transformation to their microstructure, affecting their mechanical and durability properties (Moghadam & Izadifard, 2020a). The behavior of concrete after exposure to high temperatures is critical to evaluate the residual strength and the reliability of structure for rehabilitation or destruction. However, investigating the specification of concrete exposing to high temperatures is crucial for the safety design of the members and providing a deep understanding of their behavior during the exposure to high temperatures. If the necessary measures in the design process are not taken, irreparable loss of life and property will be possible during exposure to high temperatures. Experimental studies are essential to monitoring the exact behavior of concrete elements in

*Correspondence: m.abdimoghadam@pu.ac.ir
[1] Present Address: Department of Civil Engineering, Faculty of Engineering, Pars University, Tehran, Iran
Full list of author information is available at the end of the article

these situations, however, need considerable time, cost, and may cause injury during the test. The experimental results indicated that the effect of high temperature on the mechanical properties of concrete was marginal at temperatures below 200 °C. On the other hand, significant changes were observed at temperatures above 400 °C (Uysal et al., 2012). A comparison that was made between the tensile strength and compressive strength illustrated that the vulnerability of the tensile strength owing to high-temperature exposure is greater than the compressive strength (Khaliq & Waheed, 2017). Therefore, improvement and prediction of the tensile strength are crucial. The tensile strength of concrete after high-temperature exposure, which illustrates the residual tensile strength of concrete was investigated in previous studies (Khaliq & Waheed, 2017; Uysal et al., 2012). However, a few studies focused on the tensile strength of concrete during exposure to high temperatures (Bamonte & Gambarova, 2012; Izadifard et al., 2021a; Novak & Kohoutkova, 2018; Novák & Kohoutková, 2017). The results of the tensile strength test on cooled specimens showed that no changes were observed for the tensile strength up to 200 °C (Abdelrahim et al., 2021). In contrast, the experimental test on the tensile strength of the normal, high strength, and pozzolanic concrete during exposure to high temperatures showed severe damage at temperatures below 200 °C (Izadifard et al., 2021a, b; Mehrdad Abdi Moghadam, 2019). The vulnerability of the tensile strength of concrete to high temperatures has led researchers to make efforts to improve this characteristic of concrete exposed to high temperatures. One of the solutions to improve concrete behavior during exposure to high temperatures is the inclusion of fibers in concrete (Moghadam & Izadifard, 2020b). Steel fiber possesses a high melting point and supports the structure of concrete at high temperatures by bonding effect. Mehdipor et al. demonstrated that increasing the amount of steel fiber in the mix leads to an increase in tensile strength (Mehdipour et al., 2020). Rao and Narayana reported that steel fiber improved the compressive, tensile, and flexural strength in the range of 6–10, 0–12, and 0–20%, respectively, at temperatures ranging from 50 to 250 °C (Rao & Narayana, 2013). One of the factors affecting the productivity of the fiber on the specifications of the concrete after exposure to high temperatures is the dosage of fiber (Ahmad et al., 2019; Liu et al., 2020). Ali et al. incorporated a range of 0.05–2% of steel fibers to investigate the compressive and tensile strength of concrete at ambient temperature. They showed that the optimum content for compressive strength was 0.25% (Ali et al., 2020).

As mentioned earlier, the study of the tensile strength of concrete at the hot state has been less studied. Novak and Kohoutkova illustrated that the tensile strength at

400 and 600 °C is 0.6 and 0.3 of the tensile strength at ambient temperature (Novák & Kohoutková, 2017). The influence of steel and polypropylene fiber on the properties of normal concrete subjected to the ISO 834 fire was studied by Yermak et al. (2017). They revealed that specimens containing a higher dosage of steel fibers experienced spalling. Drzymała et al. studied the effect of high temperature on the mechanical and physical properties of concrete at temperatures of 300, 450, and 650 °C (Jackiewicz-Rek et al., 2016). The results showed that the compressive strength at a temperature of 300 °C was higher than that of at the ambient temperature. In this regard, Abdi Moghadam and Izadifard (Mehrdad Abdi Moghadam, 2019) reported an increase of the compressive strength at temperatures of 400 °C for normal and pozzolanic concrete. A deep investigation on the microstructure of mortar showed that the internal curing effects of the mortars at these temperatures caused this rise of strength (Moghadam & Izadifard, 2020a).

Lack of knowledge in the properties of concrete during high temperatures exposure could result in financial damages and life-threatening events. Therefore, there is a need for a comprehensive model, to predict the tensile strength of concrete. An efficient and reliable model for estimating the tensile strength of concrete with the risk of high-temperature exposure can help to a safe and reliable structural design. In this regard, the estimation of the mechanical properties after high-temperature exposure was introduced by Marques et al. (Marques et al., 2013). In this study, specimens were tested at temperatures of 400, 600, and 800 °C after being heated under the ISO 834 time–temperature curve. In another study that tested the concrete under high temperature, a mathematical equation for the prediction of the compressive and tensile strength of concrete was proposed. They studied the performance of concrete at elevated temperatures in the temperature range of 23–800 °C and showed that an increase in temperature causes a loss of strength. (Khaliq & Waheed, 2017). Furthermore, a model for the prediction of the splitting tensile strength of concrete after being exposed to elevated temperatures was proposed (Gao et al., 2012). In another study by Abdi Moghadam and Izadifard (2019), an equation for the estimation of the shear strength of normal and steel fiber reinforced concrete at temperatures range of 28 to 800 °C was proposed. This equation was able to predict the shear strength of concrete at the ambient temperature more accurately than the previous equation, and predict the shear strength of plain and steel fiber reinforced concrete at each temperature.

By reviewing the literature, it is concluded that the experimental data on the tensile strength of steel fiber reinforced concrete during exposure to various

temperatures is rare. Although experimental efforts have been carried out in the literature to provide data on the post-heating behavior of plain concrete and there are some models, an efficient model to predict the tensile strength of plain and steel fiber reinforced concrete (SFRC) under high-temperature exposure was not proposed. Hence, the main purpose of this study is to add robust results to the literature and propose an efficient equation to predict the tensile strength of concrete in these situations. For this purpose, a comprehensive investigation on the effects of high temperatures on the tensile strength of SFRC through experiment is conducted at temperatures of 28–800 °C, and equations based on the experimental findings to predict the tensile strength of plain and SFRC under high temperatures are developed. Finally, the proposed models are validated using test data obtained from other literature.

2 Experimental Work
2.1 Material Properties
The cementitious material in this study was ordinary type 2 Portland cement, and the characteristics of cement are shown in Table 1. Fine aggregates were river sand with a maximum size of 4 mm and a specific gravity of 2.81.

Table 1 Characteristics of the cement.

Characteristics		Results
Mineralogical Composition of Clinker	$C_3S\ C_3S(\%)$	52.67
	$C_2S\ C_2S(\%)$	19.89
	$C_2A\ C_2A(\%)$	6.09
	$C_4AF\ C_4AF(\%)$	11.74
Setting Time (Minutes)	Initial	186
	Final	276
Compressive Strength (MPa)	2 days	16.1
	3 days	23.6
	7 days	31.9
	28 days	50
Physical Properties	Fineness by Blaine Test (cm^2/gr)	3165
	Autoclave Expansion (%)	0.17

Natural coarse aggregates were calcareous and had a maximum particle diameter of 19 mm. The steel fibers were hooked end with a length of 30 mm, an aspect ratio of 37.5, and a tensile strength of 1100 MPa. The shape of fibers at temperatures of 28, 500, 650, and 700 °C, is illustrated in Fig. 1. It is seen that the appearance of steel fibers does not change at temperatures below 500 °C. An increase in temperature causes the oxidation and loss of the surface area of fibers, which results in loss of interfacial adhesion of fibers.

2.2 Experimental Procedure
In this study, the effect of steel fibers on the tensile properties of normal strength concrete (N) was investigated to develop an equation for the prediction of the tensile strength of steel fiber reinforced concrete exposing to high temperatures. To this purpose, the inclusion of steel fibers was studied and compared with plain concrete (N). The volume fraction of steel fiber in concrete's mix was 0.25% (St25) and 0.5% (St50) (equal to 19.62 and 39.24 kg/m3, respectively). The properties of the mixture with the corresponding labels are presented in Table 2, in which they were mixed and cured following ASTM C192 (2012). In the first stage of the mixing plan, the aggregates and cement were added and mixed with one-third of the mixing water for 2 min. Then, the fibers were added gradually to the running mixer and mixed for 3 min. Finally, the remained water was poured into the mixture and mixed for a further 2 min to achieve a homogeneous mix. For each mixture, three cubic specimens for the compressive strength and three cylindrical specimens for the tensile strength were cast, and the mean of those was presented. All specimens were cast, demolded after 24 h, and then submerged in the water bath at 24 ± 2 °C for 28 days. Before setting out the heating procedure, all the specimens were stored in a laboratory at a temperature of 25–30 °C and 50–60% relative humidity for 14 days to avoid explosive spalling as a result of excessive moisture.

2.3 Heating Regimes
Because higher content of free water in specimens causes spalling during the heating process, they were cured in
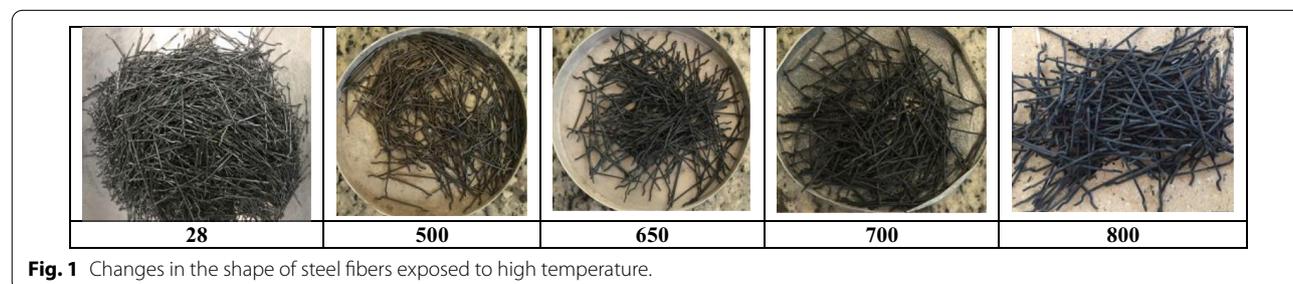

| 28 | 500 | 650 | 700 | 800 |

Fig. 1 Changes in the shape of steel fibers exposed to high temperature.

Table 2 Mixing plan.

Mixture	Concrete Component (kg/m^3)							Slump(mm)
	Portland cement	Water	Coarse aggregate	Fine aggregate	Steel Fiber	Silica Fume	Superplasticizer	
Normal Concrete (N)	400	200	935	765	_	_	_	38
High Strength Concrete(HS)	530	185	1030	700	_	50	4	25
Steel fiber concrete (St25)	400	200	935	765	19.62	_	_	26
Steel fiber concrete (St50)	400	200	935	765	39.24	_	_	15

the laboratory environment for 14 days after removing them from the water tank. This technique is confirmed by previous researchers (A. C192 & C192M, 2012; Farzadnia et al., 2013; Khaliq & Waheed, 2017; Liu et al., 2020; Marques et al., 2013). The heating of specimens was conducted after 42 days of casting, and tests were conducted at a hot state. The rate of heating was 1–3 °C/min. To ensure a steady-state thermal condition throughout the specimens, when the temperature reached the target temperature, they were maintained in the furnace for 180 min. All of the tests were performed immediately after removing them from the furnace, and these tests were carried by a 3000 KN testing machine. Although a temperature drop occurs after leaving the furnace, this is negligible for the core of specimens (Moghadam & Izadifard, 2020b). In a laboratory study by Mydin and Wang, concrete temperatures throughout the testing period as reported almost constant. The results showed that the temperature drop of the concrete core after 1 min was 0.5 °C (Mydin & Wang, 2012). Novak and Kohoutkova suggested that to avoid excessive temperature loss, the time of the test after removing specimens from the furnace should be under 10 min (Novák & Kohoutková, 2017). References (Rao & Narayana, 2013) and (Faiyadh & Al-Ausi, 1989) also examined the characteristics of

concrete in hot conditions by this procedure. In this study, this duration is in the range of 1–3 min.

2.4 Testing Method
The compressive and tensile strength tests were conducted according to British standard (2009) and ASTM C 496 (2004), respectively. To prevent temperature drop, immediately after finishing the heating procedure, the specimens were removed from the furnace by a steel paddle and placed on a moving table to transfer near the jack. Then, they were placed under the jack using high-temperature resistant gloves and a trowel. Afterward, compressive and tensile strength was performed. Fig. 2 shows the detail of the apparatus and test process.

3 Results and Discussion
3.1 The Effect of Steel Fiber on the Mechanical Properties
The experiments on the specimens at the ambient temperature are conducted after 28 and 42 days of curing. The experimental results which are the average of three replicate, the coefficient of variation (C.o.V.), and the standard deviation (St. Dev.) are listed in Table 3. It is seen that the incorporation of 0.25% and 0.5% of fibers can provide an increase of 24.53% and 22.37% for the tensile strength of 28 days. The corresponding improvement
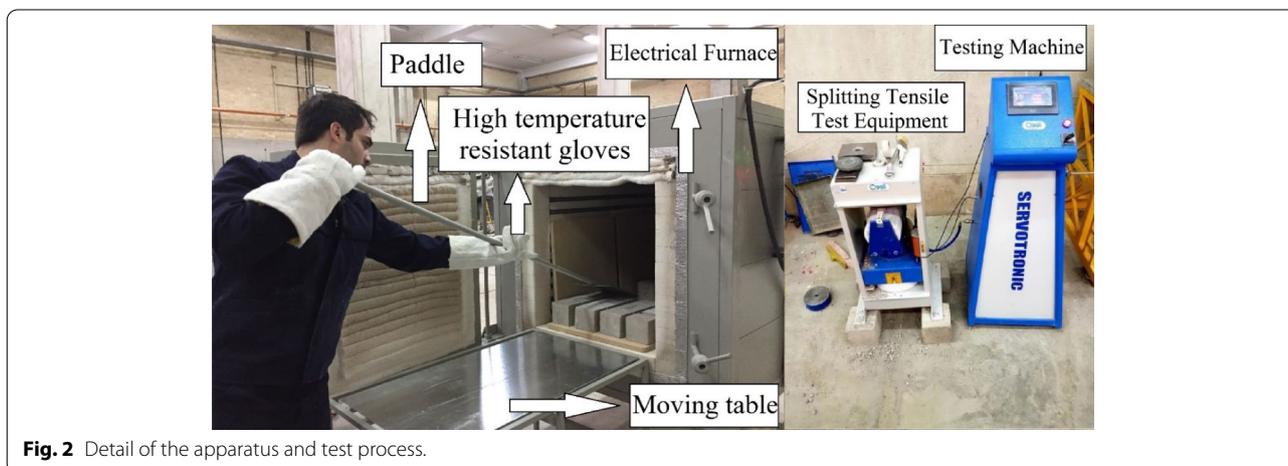

Fig. 2 Detail of the apparatus and test process.

Table 3 Compressive and tensile strength of specimens at ambient temperature.

Specimen ID	Day of test	Compressive Strength [MPa]	St.Dev [MPa]	C.o.V [%]	Tensile Strength [MPa]	St.Dev [MPa]	C.o.V [%]
N	28	47.2	0.78	1.66	2.57	0.06	2.43
N	42	53.4	2.70	5.06	3.03	0.26	8.67
St25	28	44.5	5.30	11.92	3.2	0.11	3.63
St25	42	52.6	1.89	3.59	3.88	0.19	4.9
St50	28	44.0	3.47	7.89	3.15	0.12	3.94
St50	42	52.3	0.40	0.76	3.83	0.09	2.42
HS	28	80.2	4.27	5.33	4.8	0.16	3.43
HS	42	84.5	2.38	2.82	5.2	0.15	2.97

for 42 day specimens is 28.15% and 26.32%, respectively. Steel fibers limit hair cracks expansions and improve tensile strength. During the splitting of specimens, the stress transfers from the cement matrix to fibers and improves the tensile strength of concrete. On the other hand, the incorporation of steel fibers has provided a loss of compressive strength. The results show that the compressive strength of St25 after 28 and 42 curing days is 5.75 and 1.53% lower than normal concrete. The incorporation of 0.5% of steel fibers decreases the 28 day and 42 day compressive strength of normal concrete by 6.79 and 1.96%. The addition of steel fibers causes a reduction in workability, which leads to inadequate compaction. In addition, a balling effect resulting from the non-uniform distribution of fibers leads to detachment of the concrete structure. These issues seem to be the reasons for the loss of compressive strength. Moreover, it is observed that an increase of the compressive strength from 40 to 80, has increased the tensile strength by 86.51%.

3.2 Tensile Strength of Plain Concrete

To propose an equation for prediction of the tensile strength, a specimen with a compressive strength of 20.1 and a tensile strength of 1.93 MPa was prepared. All of the cubic compressive strength were converted to the standard cylindrical compressive strength and are plotted in Fig. 3. In this figure, the correlation between the tensile strength and compressive strength is plotted. Using regression analysis, an equation is proposed with a high coefficient of determination ($R^2 = 0.88$). This shows a strong relationship between the tensile strength (f_t) and the compressive strength (f_c).

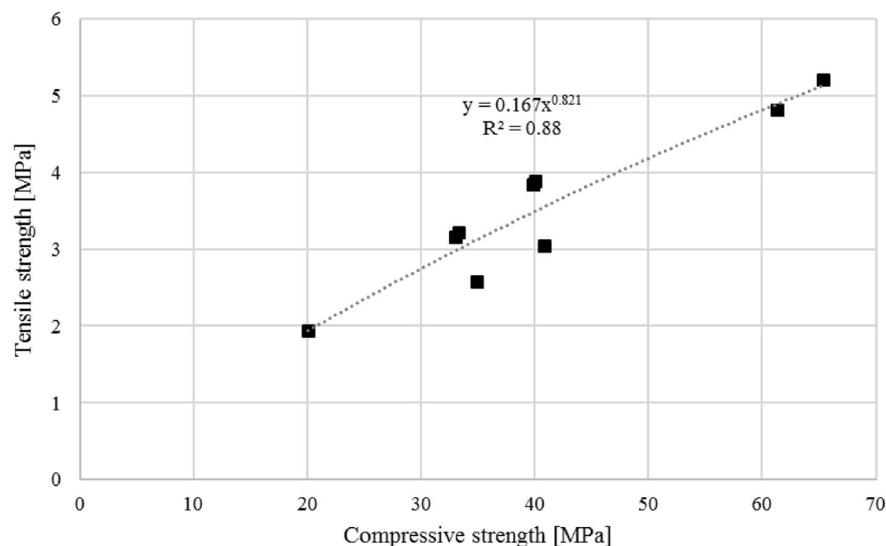$$f_t = 0.167 f_c^{0.821} \quad R^2 = 0.88 \qquad (1)$$

Fig. 3 Correlation between the tensile strength ($\boldsymbol{f_t}$) and the compressive strength ($\boldsymbol{f_c}$).

Table 4 lists the previous equations for the estimation of the tensile strength of normal concrete (A.C., 1984; Astm, 2004; Faiyadh & Al-Ausi, 1989; Guide & Manual, 2005; Hueste et al., 2004; Müller & Hilsdorf, 1990; Mydin & Wang, 2012; Perumal, 2014; Rashid et al., 2002; Standard, 2009; Wafa & Ashour, 1992). To compare Eq. 1 with the previous equations, they are plotted in Fig. 4. This figure shows that the evaluated tensile strength for specimens with compressive strengths lower than 40 MPa is lower than other equations. For compressive strength in the range of 40–60 MPa, Eq. 4 is most consistent with previous relationships. For specimens with compressive strength higher than 60 MPa, the proposed equation in this study is lower than the equations reported in references (Hueste et al., 2004; Müller & Hilsdorf, 1990; Thomas & Ramaswamy, 2007). In contrast, the value obtained by Eq. 1 is higher than other equations.

To verify the accuracy of Eq. 1, 72 experimental data from 27 previous studies (Bani-Yasin, 2004; Craig et al., 1986; El-Niema, 1991; El-SAYAD & EFFECT, 2005; Kwak et al., 2002; Marar & Celik, 2002; Mitchell et al., 1996; Nadiya & Saffar, 2006; Narayanan & Kareem-Palanjian, 1983; Patel et al., 2017; Ramadoss, 2014; Rao, 2016; Rjoub & Muhammad, 2006; Sarbini et al., 2013; Sharma, 1986; Singh et al., 2016; Song & Hwang, 2004; Srikar & Kalyan, 2018; Sumathi & Saravana, 2014; Vairagade et al., 2012; Wadekar & Pandit, 2014; Yan et al., 2013) are collected ($f_{t_{exp}}$. The lowest and highest compressive strengths of the selected data are 18.1 and 98.92 MPa, respectively. Using the experimental compressive strength (f_c) and Eq. 1, $f_{t_{calc}}$ is calculated. To evaluate the accuracy of this equation, the correlation of the predicted tensile strength with the experimental results of previous researchers is shown in Fig. 5. In this figure, the horizontal axis shows the experimental tensile strength and the vertical axis

Table 4 Previous equation for estimation of the tensile strength of concrete at ambient temperature.

Reference	Equation [MPa]	Reference	Equation [MPa]
CEB_FIP (1990)	$f_t = 0.3 f_c^{0.67}$	Hueste et al .(2004)	$f_t = 0.55 f_c^{0.5}$
ACI 363R-92 (1984)	$f_t = 0.59 f_c^{0.5}$	Thomas and Ramasamy (2007)	$f_t = 0.57 f_c^{0.5}$
ACI318-99 (2005)	$f_t = 0.56 f_c^{0.5}$	Xu and Shi (2009)	$f_t = 0.21 f_c^{0.83}$
Ahmad and Shah (1985)	$f_t = 0.46 f_c^{0.55}$	Ramadoss (2014)	$f_t = 0.12 f_c^{0.95}$
Wafa and Ashou (1992)	$f_t = 0.58 f_c^{0.5}$	Choi and yuan (2005)	$f_t = 0.6 f_c^{0.5}$
Rashid et al. (2002)	$f_t = 0.47 f_c^{0.56}$	Perumal (2014)	$f_t = 0.188 f_c^{0.84}$

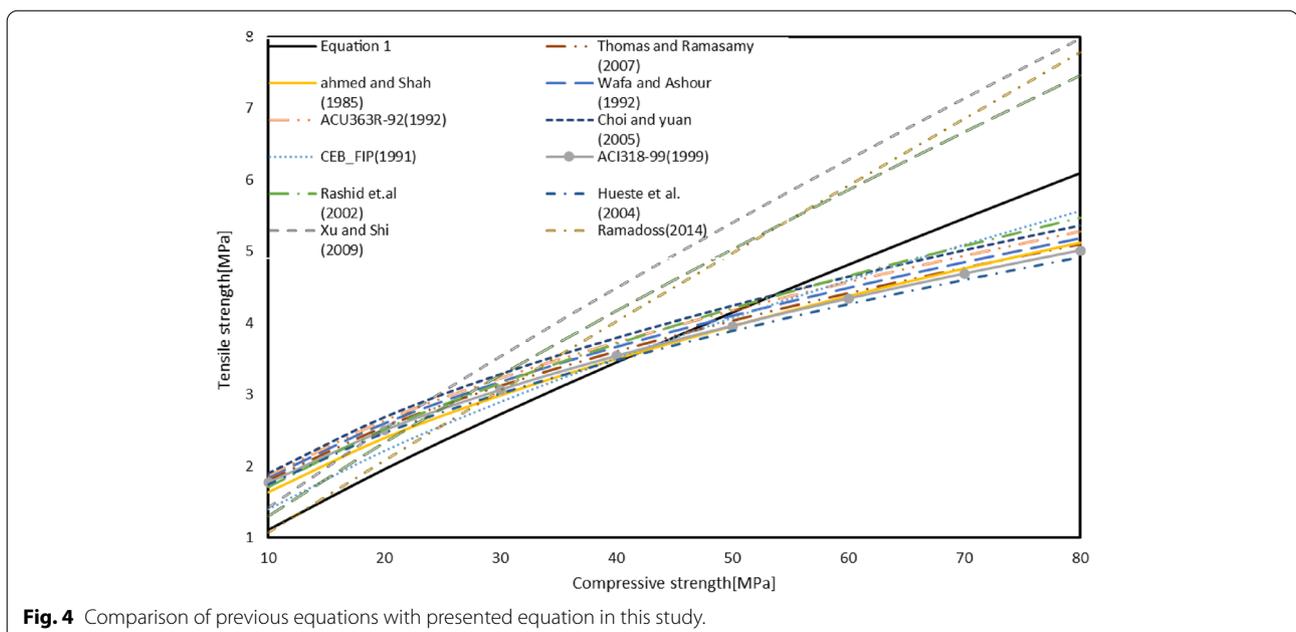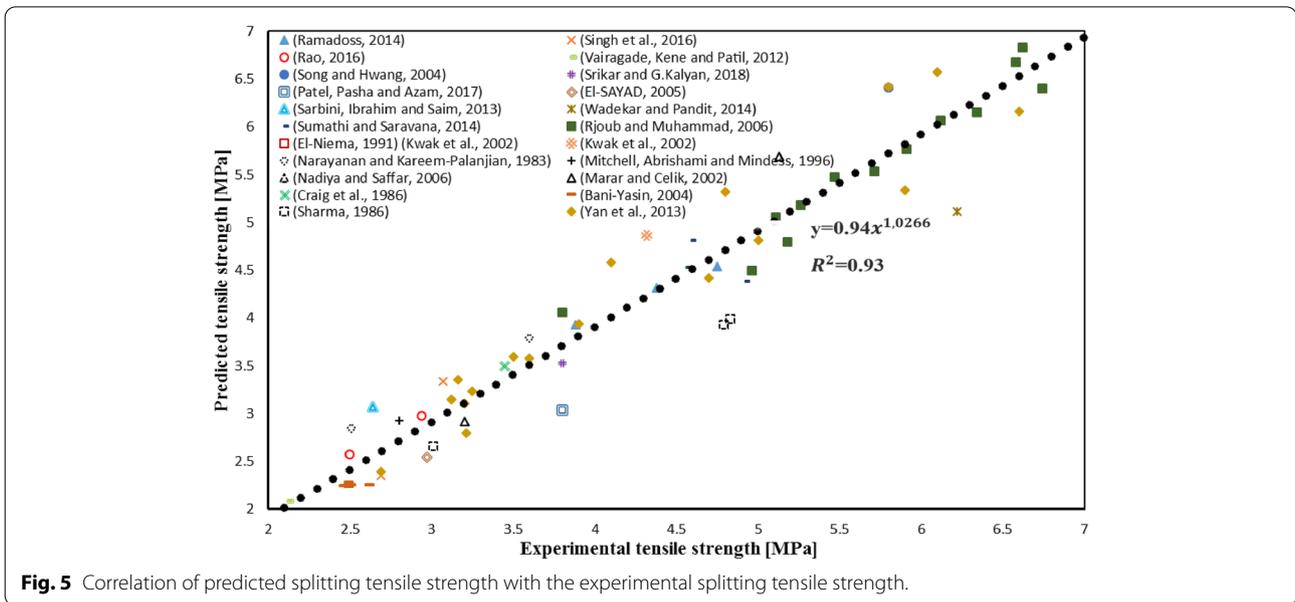f_c The cylindrical compressive strength of plain concrete (MPa)

Fig. 4 Comparison of previous equations with presented equation in this study.

Fig. 5 Correlation of predicted splitting tensile strength with the experimental splitting tensile strength.
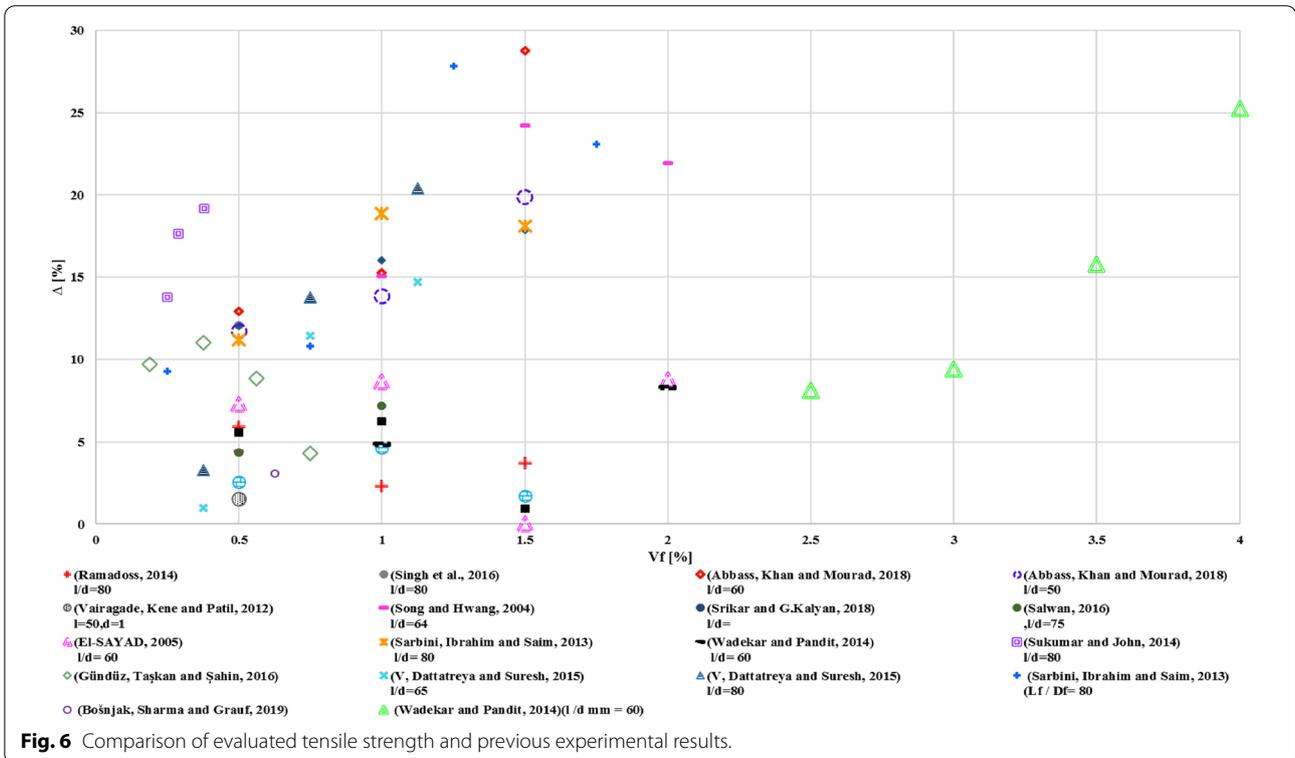
shows the calculated tensile strength. Using regression analysis, a strong equation with a high coefficient of determination ($R^2 = 0.93$) is obtained. This graph illustrates a strong correlation between the evaluated and experimental results. Examination of these 72 cases show that the average difference between the evaluated and experimental tensile strength is 7.53%, which describes the accuracy of the equation.

3.3 Tensile Strength of Steel Fiber Reinforced Concrete

To determine the tensile strength of the steel fiber reinforced concrete, the contribution of fibers ($f_{t(f)}$) is summed to the tensile strength of plain concrete ($f_{t(c)}$). Equation (2) illustrates the tensile strength of the steel fiber reinforced concrete:

$$f_{t(\mathrm{FRC})} = f_{t(c)} + f_{t(f)} \tag{2}$$

Fig. 6 Comparison of evaluated tensile strength and previous experimental results.

By conducting the regression analysis on the experimental data presented in Table 3, $f_{t(f)}$ is obtained in the form of the following equation:

$$f_{t(F)} = 1.59V_f \tag{3}$$

where V_f is the volume fraction of steel fiber. By substituting Eq. (3) in Eq. (2), the tensile strength of steel fiber reinforce concrete is calculated by the following equation:

$$f_{t(\mathrm{FRC})} = f_{t(c)} + 1.59V_f \ (\mathrm{MPa}) \tag{4}$$

To evaluate the validity of this equation, the experimental results from previous studies are gathered (Abbass et al., 2018; Bošnjak et al., 2019; El-SAYAD & EFFECT, 2005; Gündüz et al., 2016; N. V, J.K. Dattatreya & S. Suresh, 2015; Ramadoss, 2014; Salwan & EFFECT, 2016; Sarbini et al., 2013; Singh et al., 2016; Song & Hwang, 2004; Srikar & Kalyan, 2018; Sukumar & John, 2014; Vairagade et al., 2012; Wadekar & Pandit, 2014) and compared with the calculated tensile strength using Eq. (4). In this aim, the selected data are for specimens containing a wide range of volume fractions ($0.25 \le V_f \le 4\%$). To evaluate the accuracy of this equation, Fig. 6 which illustrates the difference between the evaluated and experimental results is presented. The horizontal axis shows the volume fraction of fibers, and the vertical axis shows the difference between the calculated and experimental data (Δ). The difference between the calculated tensile strength and experimental results of specimens containing various content of steel fibers is in the range of 0.95–28.76%, and the average deviation is around 11%. Based on these results it is observed that the deviation of the calculated and experimental tensile strength is in an acceptable range. The deviation of the proposed model from experimental results of Wadekar and Pandit, (2014) for volume fractions of 1, 2, 2.5, 3, 3.5, and 4 is 4.83, 8.39, 8.11, 9.41, 15.77%, 25%, and 24%, respectively. This comparison with the experimental results of Ramadoss (2014) (1.72%), Vairagade (2012) (1.57%), and Bošnjak (2019) (3.06%) is marginal. Overall, the average deviation of the model from 62 test data is 11%, which indicates the high accuracy of Eq. 4. These differences are attributed to the specifications of fibers (type and aspect ratio), aggregate size, and the compressive strength of reference concrete.

Substitution of Eq. (1) into Eq. (4) yields the following equation:

$$f_{t(\mathrm{FRC})} = 0.167f_c^{0.821} + 1.59V_f \quad (\mathrm{MPa}) \tag{5}$$

where f_c is the cylindrical compressive strength [MPa] and V_f is the volume fraction of the steel fiber [%]. 50 experimental data from 14 earlier studies (Bošnjak et al., 2019; El-Sayad & Effect, 2005; Gündüz et al., 2016; Mansur et al., 2008; N. V, J.K. Dattatreya & S. Suresh, 2015;

Ramadoss, 2014; Sarbini et al., 2013; Singh et al., 2016; Song & Hwang, 2004; Srikar & Kalyan, 2018; Sukumar & John, 2014; Wadekar & Pandit, 2014) are used to verify Eq. 5. The deviation between the evaluated and experimental results is plotted in Fig. 7. The average deviation of this model from experimental data is 11%, which indicates the high accuracy of Eq. (5).

3.4 The Tensile Strength of Normal Concrete Exposed to High Temperatures

To develop Eq. (5) for high temperatures, the tensile strength of normal concrete at high temperatures is linked to the tensile strength at ambient temperature using λ_T function in the form of the following equation:

$$f_{t(T)} = \lambda_T f_{t(a)} \tag{6}$$

where $f_{t(T)}$ is the stensile strength of normal concrete at high temperature, $f_{t(a)}$ is the tensile strength of normal concrete at ambient temperature, and λ_T is a function of temperature which considers the effect of temperature on the tensile strength of normal concrete. Regression analysis was carried out on the $f_{t(T)}/f_{t(a)}$.

(Listed in Table 4) and temperatures to obtain λ_T which is expressed by Eq. (7). The experimental results with the corresponding (C.O.V.) and (St. Dev.) are shown in Table 5.

$$\lambda_T = 1.514 \times 10^{-5}T^2 - 6.76 \times 10^{-3}T + +1.18$$
$$T \le 400 \quad R^2 = 0.88$$
$$\lambda_T = 3 \times 10^{-6}T^2 - 4.62 \times 10^{-3}$$
$$T + 2.02 \ \mathrm{T} > 400 R^2 = 0.95 \tag{7}$$

A comprehensive review of past studies has shown that limited equations have been proposed for the prediction of the tensile strength at high temperatures. These equations are presented in Table 6 and are plotted in Fig. 8. In this table, the temperature ranges in which these relationships are valid and the type of the test is provided (hot or cooled state). In Fig. 8, the experimental results of the normalized tensile strength which is as λ_T are also presented. Blue and red values illustrate the cooled and hot state conditions, respectively.

It can be seen that at temperatures below 300 °C, the experimental tensile strength at the hot state is lower than the residual tensile strength. This can be attributed to the effect of internal pressure resulting from the evaporation of free water. Furthermore, it is seen that an increase of the tensile strength at temperatures of 300–400 °C is seen for tests at a hot state. Novak (2017) and Faiyadh (1989) which tested the tensile strength of concrete at hot state, reported an increase of λ_T at temperatures of 350 and 400 °C, respectively. The lack of this
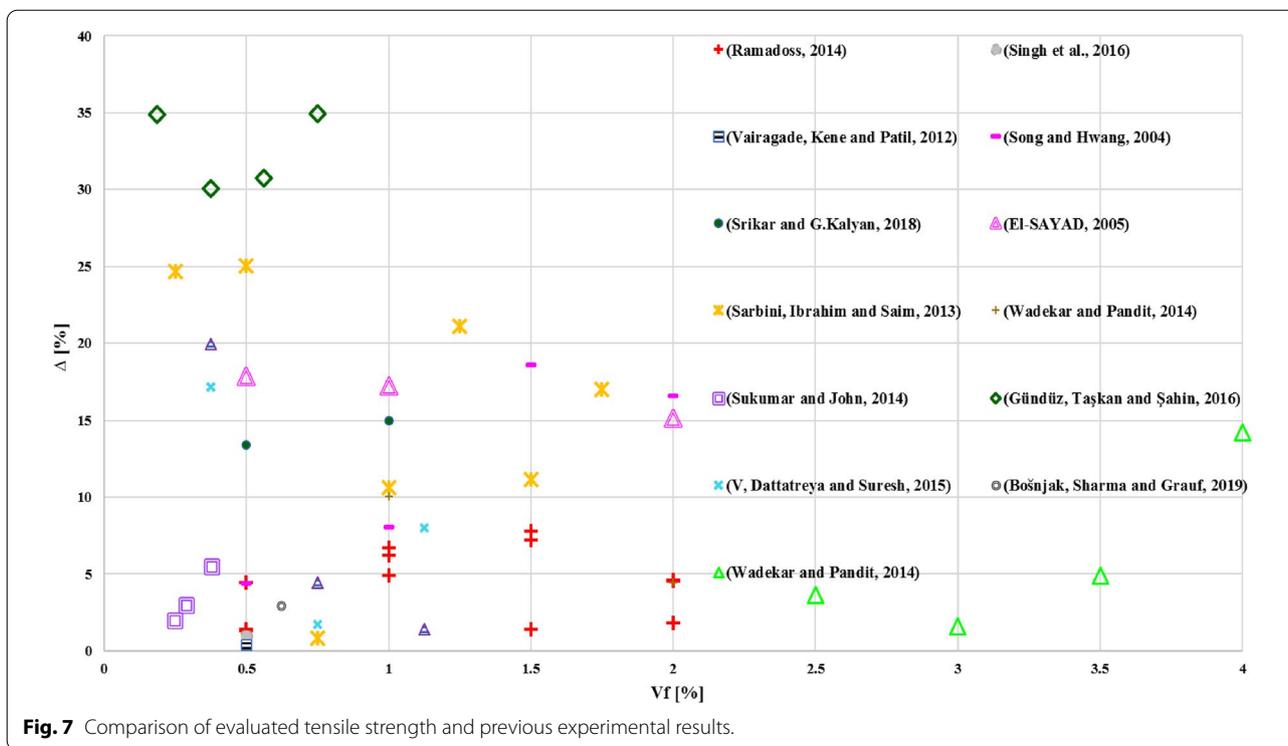
Fig. 7 Comparison of evaluated tensile strength and previous experimental results.

Table 5 Experimental results and evaluated tensile strength.

Temperature (°C)	Experimental Tensile Strength [MPa]	St.Dev [MPa]	C.o.V [%]	Evaluated Tensile Strength [MPa]	Δ[%]
28	3.03	0.26	8.67	3.03	− 0.01
100	2.11	0.18	8.39	1.98	− 6.32
200	0.92	0.05	5.8	1.30	41.44
300	1.85	0.24	12.91	1.54	− 16.68
350	2.16	0.12	5.74	2.00	− 7.19
400	2.52	0.24	9.46	2.70	7.03
450	1.55	0.14	9.32	1.67	7.43
500	1.51	0.34	23.28	1.40	− 7.53
650	0.75	0.06	8.01	0.86	14.99
800	0.69	0.03	4	0.74	6.93

increase in Rao and Khaliq studies () is due to the absence of experimental data in these temperature ranges. For example, Rao et al. tested the tensile strength of concrete in the hot state up to 250 °C, and in studies of Khaliq et al. (2017) tests were not conducted at a temperature of 200 to 400 °C. However, for specimens which tests were conducted after cooling (Khalil, Kim, Abaeian, Bošnjak, Gao, Bastami) (Abaeian et al., 2018; Bastami et al., 2014; Bošnjak et al., 2019; Gao et al., 2012; Khalil, 2018; Kim & Lee, 2015), a descending trend for the residual tensile

strength was reported. Based on this figure, it is seen that Eq. (7) provides the lowest value at temperatures range of 100–300 °C. At a temperature of 100 °C, the proposed model in this study has a slight difference from the experimental results of Khaliq and Waheed (Khaliq & Waheed, 2017). This comparison at a temperature of 200 °C, shows a minor deviation from the experimental results of Novak and Kohoutkova (Novák & Kohoutková, 2017). The experimental tensile strength reported by Rao et al. (Rao & Narayana, 2013) has a negligible deviation with the evaluated tensile strength at a temperature of 250 °C. The free water is evaporated at a temperature of 350 °C. Therefore, the proposed model based on the test at the hot state is almost consistent with the previously proposed model (Bažant & Chern, 1987; E.C. for S. (CEN) 1992; Gao et al., 2012; Chang et al., 2006; Zaici, 1998). Meanwhile, the comparison of the proposed model with the experimental result at the hot state shows that at a temperature of 600 °C, the evaluated and experimental tensile strength of Faiyadh (1989) is the same. These comparisons show that Eq. 7 estimates the overall trend of the normalized tensile strength of concrete with high accuracy.

The evaluated tensile strength using Eq. 6, and the deviation of the evaluated tensile strength from experimental results are presented in Table 5. It is seen that the average deviation of the evaluated and experimental data is 11.55%, which illustrates the high accuracy of this equation. Fig. 9

Table 6 Previous tensile strength equation at/after high-temperature exposure.

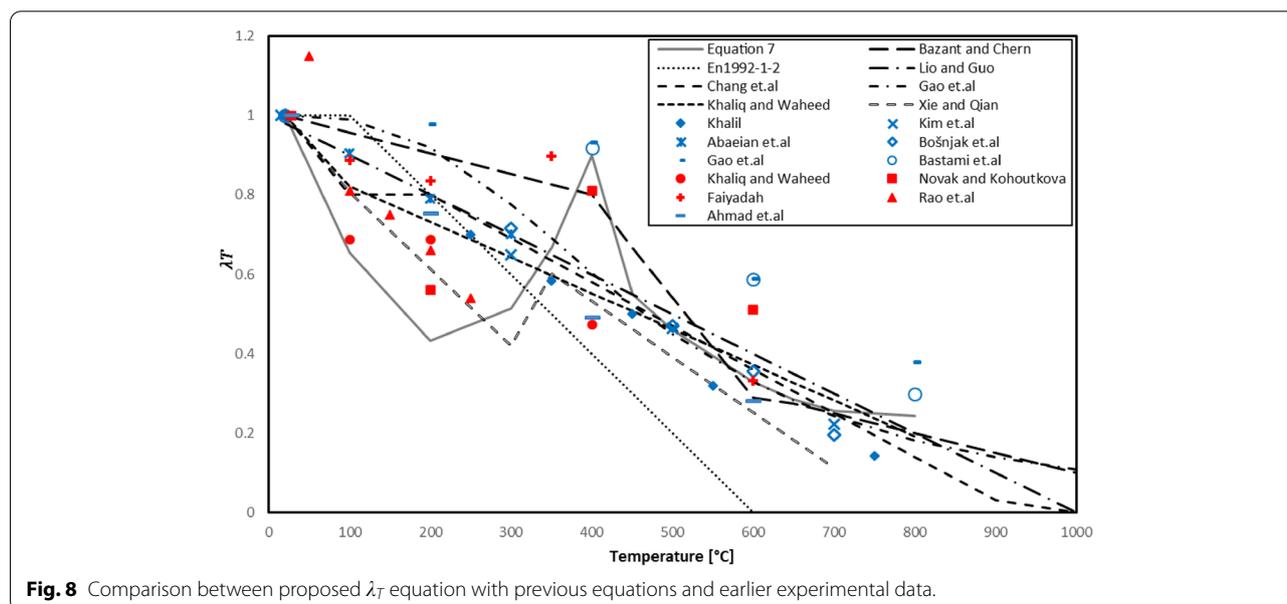| Reference	Equation	Temperature Range	Hot/Cooled
Bazant and Chern (1987)	$-0.000526\,T+1.01052$ $20\,°C \leq T \leq 400\,°C$ $-0.00252\,T+1.8$ $400\,°C \leq T \leq 600\,°C$ $-0.0005\,T+0.6$ $600\,°C \leq T \leq 800\,°C$	$20\,°C \leq T \leq 800\,°C$	Cooled
Gao et.al (2012)	$\dfrac{1}{1+8\times10^{-8}(T-20)^{2.68}}$	$20\,°C \leq T \leq 800\,°C$	Cooled
En1992-1–2 (1992)	1 $20\,°C \leq T \leq 100\,°C$ $1-(\frac{T-100}{500})$ $400\,°C \leq T \leq 600\,°C$ 0 $600\,°C \leq T$	$20\,°C \leq T \leq 1000\,°C$	Cooled
Chang et al. (2006)	$1.05-0.0025\,T$ $20\,°C \leq T \leq 100\,°C$ 0.8 $100\,°C < T \leq 200\,°C$ $1.02-0.0011\,T$ $600\,°C < T \leq 800\,°C$	$20\,°C \leq T \leq 800\,°C$	Cooled
Xie and Qian (1998)	$0.58\times(1-\frac{T}{300})+0.42$ $20\,°C \leq T \leq 300\,°C$ $0.42\times(1.6-\frac{T}{300})+0.42$ $300\,°C \leq T \leq 800\,°C$	$20\,°C \leq T \leq 800\,°C$	Cooled
Li and Guo (1993)	$1-0.001\,T$	$20\,°C \leq T \leq 1000\,°C$	Hot
Khaligh and Waheed (2017)	$0.9118-0.0009\,T$	$23\,°C \leq T \leq 800\,°C$	Hot

Fig. 8 Comparison between proposed λ_T equation with previous equations and earlier experimental data.

illustrates the failure modes of fractured surfaces at temperatures of 450, 650, and 800 °C. It is seen that aggregates have a great role in the tensile strength behavior of concrete at temperatures below 500 °C. However, at temperatures above 500 °C, the expansion of cracks in the microstructure and incompatibility of the coefficient of thermal expansion breeds the detachment of aggregates. Owing to these justifications, the number of aggregates that contribute to load barring decreases. Furthermore, the red surface of fractured specimens at temperatures of 800 °C illustrates that tests were done in hot conditions.

The comparison of test data of Table 5 and evaluated results from Eq. (6) are shown in Fig. 10. It is seen that with increasing the temperature up to 200 ℃, the tensile strength of concrete fell. Previous studies have shown

that no chemical changes occur in the concrete microstructure in these temperature ranges (Kowalski, 2010). Therefore, the loss of tensile strength at these temperatures is connected to the evaporation of free water, which intensifies the internal pressure. At temperatures range of 200–400 ℃, the tensile strength increases. The hydration of un-hydrated cement owing to exposure to high temperature is attributed to this improvement (Xiao et al., 2018). An increase of surface forces between cement gel layers is another responsible factor for this improvement (Castillo, 1987). By increasing the temperature from 400 to 800 °C, chemical changes and degradation of microstructure intensifies, which results in a severe loss of tensile strength. Previous research of Abdi Moghadam and izadifard on the microstructure of mortars showed that
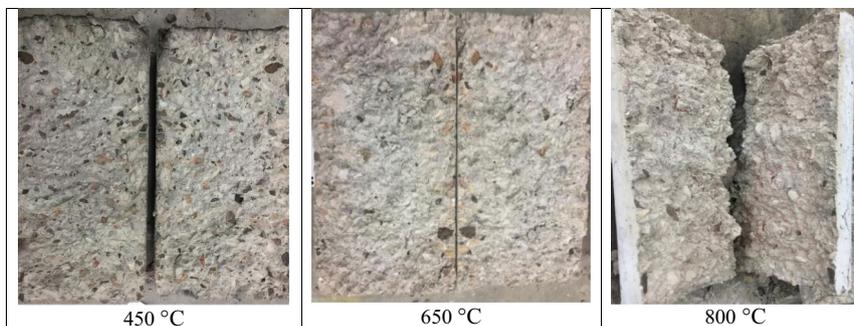
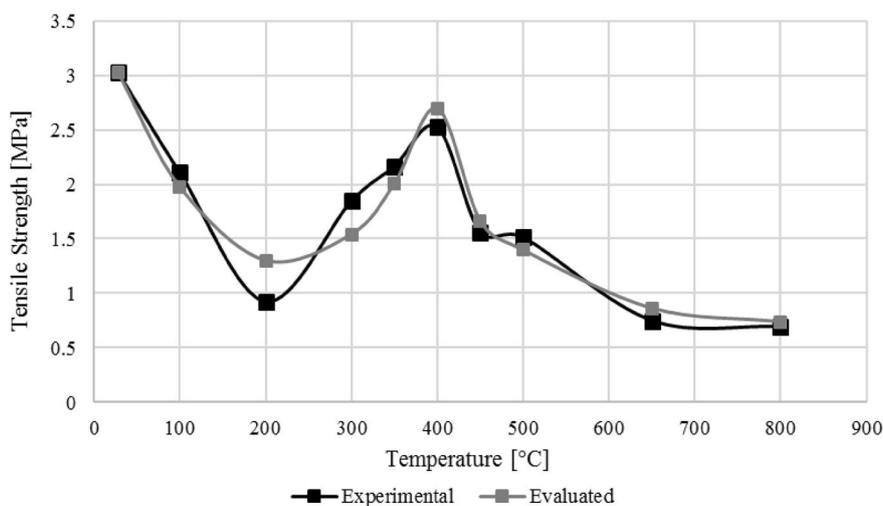**Fig. 9** Failure modes of fractured surfaces.

Fig. 10 Variation of the tensile strength at high temperatures.

the intensity of CSH peak is almost constant up to 400 °C and has dropped significantly at 800 °C. Furthermore, the calcium silicate peaks which are the product of C–S–H decomposition increased significantly at a temperature of 800 °C. Another product that was observed in XRD patterns of specimens that experienced 800 °C, is calcium silicate. It can be another reason for the sharp decrease in the mechanical properties of the mortar at this temperature. Other observations at 800 °C include a significant decomposition of calcium silicate hydrate peak and portlandite peak (Moghadam & Izadifard, 2020a). Based on this figure, it is seen that the deviation of the evaluated tensile strength from the experimental tensile strength is marginal, except at 200 °C. At 200 °C, owing to the simultaneous effect of the jack and vapor pressure resulting from the evaporation of the free water in capillary pores, a loud voice followed by the steam outlet was observed (Moghadam & Izadifard, 2020b). The average deviation

of the predicted tensile strength from experimental results at temperatures of 28–800 °C is 11.55%, illustrating the high precious of Eq. 6.

3.5 The Tensile Strength of Steel Fiber Reinforced Concrete Exposed to High Temperature

Equation (8) illustrates that the tensile strength provided by steel fibers is considered as a function of volume fractions of steel fibers. In this equation, β_T is a function of temperature considering the effect of volume fractions of steel fibers on the tensile strength of plain concrete:

$$f_{t(F)(T)} = \beta_T V_f \tag{8}$$

By calculating this coefficient at each temperature and applying a regression analysis, β_T is calculated in the form of the following equation:

$$\beta_T = -2. \times 10^{-7}T^3 + 6.14 \times 10^{-5}T^2 + 0.0062T + 1.28 \quad T \leq 400 \quad R^2 = 0.91$$
$$\beta_T = 4.21 \times 10^{-6}T^2 - 0.013T + 8.37 \quad T > 400 \quad R^2 = 0.80$$

(9)

Finally, the equation for the prediction of the tensile strength of steel fiber reinforced concrete is in the form of the following equation:

$$f_{t(FRC)(T)} = \lambda_T f_{t(a)} + \beta_T V_f \qquad (10)$$

where $f_{t(FRC)(T)}$ is the tensile strength of steel fiber reinforced concrete at high temperature.

The experimental tensile strength with the corresponding (C.O.V.) and (St. Dev.) are shown in Table 7, where they are compared with the predicted tensile strength using Eq. (10). Based on this table, it is seen that the deviation of the predicted tensile strength from the experimental values for St25 and St50 is in the range of 2.95–14.17 and 0.35–11.5%, respectively.

Fig. 11 represents changes in the tensile strength in the steel fiber-reinforced concrete at different temperatures, where they are compared with the predicted tensile strength using Eq. 10. This figure shows that the variation of the splitting tensile strength of the normal and the fiber reinforced concrete at various temperatures is almost similar. As could be observed, all specimens experienced a reduction up to 200 °C. At this temperature, the tensile strength of St25 and St50 is almost similar, and the inclusion of steel fibers improved the tensile strength of normal concrete. Interfacial adhesion and mechanical anchoring of steel fibers seem to be another reason for the increase of tensile strength. The inclusion of steel fibers allows heat to transfer easily inside the concrete, which reduces the thermal stress and the expansion of cracks. However, the rate of the tensile strength improvement is decreased at temperatures of 650 and

800 °C. This can be attributed to the effect of high temperature on the loss of bonding properties. Past studies have shown that the performance of the fibers does not change up to 500 °C and decreases at higher temperatures. The yield stress and ultimate stress of the steel fibers at 800 °C are 15% and 25% of ambient temperature, respectively (Abdallah et al., 2017). These changes in the steel fiber behavior cause the descending trend of the tensile strength at temperatures above 500 °C. Furthermore, the expansion of steel fibers creates radial cracks surrounded the steel fibers, which is another cause of the tensile strength loss.

Table 7 shows that the average deviation of the predicted tensile strength from the experimental result of St25 and St50 is 7.68 and 5.58%, respectively. Fig. 11 presents a comparison between the predicted and experimental results. The tensile strength of steel fiber reinforced concrete has a descending trend at temperatures below 200 °C. With a further increase in temperature, the tensile strength improves and reaches a peak at 350 °C. Owing to the internal curing condition, which is the reason for strength gaining at temperatures of 400 °C, portlandite is consumed to produce higher content of CSH gels. The results of XRD illustrated that by increasing the temperature from 28 to 400 °C, the intensity of $CaCO_3$ increased from 12.2% to 19.8%, which justifies the decarburization of portlandite. However, at temperatures above 350 °C, the overall trend of the tensile strength is descending. The oxidation and corrosion of steel fibers which result in a loss of cross section of steel fibers is another reason for the tensile strength loss. The

Table 7 Comparison between the experimental and predicted tensile strength.

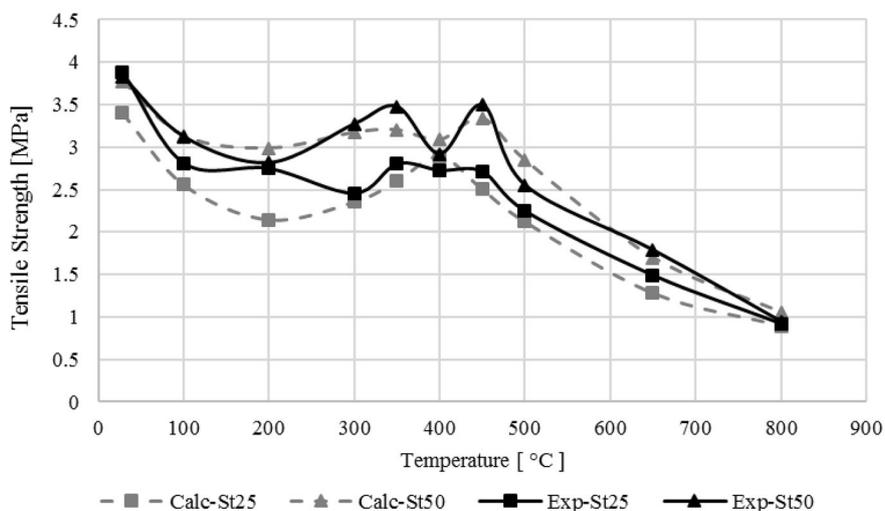| Vf [%]	0.25					0.5				
T(°C)	$f_{t_{exp}}$ [MPa]	St.Dev [MPa]	C.O.V [%]	$f_{t_{calc}}$ [MPa]	Δ[%]	$f_{t_{exp}}$ [MPa]	St.Dev [MPa]	C.O.V [%]	$f_{t_{calc}}$ [MPa]	Δ[%]
28	3.88	0.19	3.97	3.40	− 12.38	3.83	0.09	2.42	3.78	− 1.35
100	2.81	0.27	2.81	2.55	− 9.07	3.12	0.28	9.09	3.13	0.35
200	2.75	0.18	2.75	2.14	− 21.92	2.82	0.20	7.00	2.99	6.11
300	2.46	0.15	2.46	2.36	− 3.99	3.27	0.35	10.68	3.17	− 3.06
350	2.80	0.20	2.80	2.60	− 7.09	3.48	0.20	5.66	3.20	− 7.84
400	2.73	0.05	2.73	2.89	6.13	2.92	0.33	11.20	3.09	5.78
450	2.71	0.26	2.71	2.50	− 7.71	3.50	0.21	5.94	3.34	− 4.43
500	2.25	0.12	2.25	2.12	− 5.62	2.55	0.28	11.12	2.85	11.50
650	1.49	0.13	1.49	1.28	− 14.17	1.79	0.67	37.66	1.70	− 5.14
800	0.92	0.04	0.92	0.90	− 2.95	0.95	0.05	5.04	1.05	10.79

Fig. 11 Comparison between the predicted tensile strength using Eq. 10 and experimental values.

inclusion of 0.25 and 0.5% of steel fibers provide 58.48 and 80.29% improvement of the tensile strength at the tested temperatures on average. Meanwhile, the rate of increase of the tensile strength for a higher dosage of steel fibers is higher. This is due to the presence of a higher dosage of fibers at the tensile plane. Because aggregates detach from the cement matrix, the inclusion of fibers improves the tensile strength of plane concrete. Another reason for the improvement of the tensile strength owing to the inclusion of steel fibers can be attributed to the thermal conductivity of steel fibers. In specimens containing steel fibers, the heat is transferred easily which results in stress reduction. This issue reduced the crack development, and consequently the tensile strength improvement (Moghadam & Izadifard, 2020b).

To make Eq. (10) independent from the tensile strength of plain concrete at ambient temperature, and extend this equation for specimens with various compressive strength, Eq. (1) is substituted in Eq. (10):

$$f_{t(\text{FRC})(T)} = 0.167\lambda_T f_c^{0.821} + \beta_T V_f \tag{11}$$

The difference between the predicted tensile strength and experimental values is shown in Table 8. This equation not only can predict the tensile strength of steel fiber

reinforced concrete at high temperature without the tensile strength at ambient temperature but also this equation decreases the deviation of Eq. (10) at 200 °C. Based on this table, it is seen that the proposed equation can estimate the tensile strength of steel fibers reinforced concrete accurately. The average deviation of predicted tensile strength from the experimental results of St25 and St50 is 6.93% and 10.96%, respectively.

4 Conclusions

This study focused on the effects of high temperatures on the tensile strength of normal and steel fiber reinforced concrete. Based on the results presented in this paper, the following conclusions are drawn:

– The overall trend of the tensile strength of plain and steel fiber reinforced concrete followed a similar trend at high temperatures. At temperatures below 200 °C, they experienced a sudden loss which can be attributed to the simultaneous effect of the jack and the evaporation of the free water. A review of the previous experimental results illustrated this loss did not occur for specimens that were tested after exposure to high temperatures. 200 °C onward, they recover their strength because of the hydration of un-hydrated cement owing to autoclave curing con-

Table 8 Percent errors of the predicted tensile strength by Eq. 11.

Vf [%]	T (°C)	28	100	200	300	350	400	450	500	650	800
0.25	Δ[%]	− 0.07	2.04	− 14.44	5.92	4.21	21.74	1.98	4.19	− 5.05	9.67
0.5	Δ[%]	11.14	10.35	13.41	4.37	1.27	20.36	3.09	20.14	2.46	23.05

dition. On the other hand, a further increase in temperature resulted in a descending trend in the tensile strength of the plain and steel fiber reinforced concrete.

– The incorporation of steel fiber improved the tensile strength of plain concrete under high-temperature exposure. The inclusion of 0.25 and 0.5% steel fibers improved the tensile strength of specimens at elevated temperatures averagely by 58.48% and 23.81%. These values are valid for concrete containing hooked end steel fibers.

– The compressive strength has a great impact on the tensile strength of concrete, where an increase of compressive strength from 20.1 to 84.45 improves the tensile strength by 169.4% at ambient temperature. Using experimental data of this study and conducting regression analysis, an equation with high accuracy for the prediction of the tensile strength of normal concrete at ambient temperature is proposed. A comparison of the proposed equation in this study with the previous equations shows that this equation is most consistent with the previous equations in the compressive strength range of 40–60 MPa. Further verification of this equation by comparing the evaluated tensile strength with the previous experimental results reveals the average deviation of the predicted tensile strength from the experimental values is 7.53%, which describes the accuracy of the equation. This equation is developed to predict the tensile strength of steel fiber reinforced concrete at ambient temperature. The validity of this equation is verified by comparing the predicted tensile strength from previous experimental data having a wide range of volumes fractions (0.25–4%). The average deviation of the predicted tensile strength from the experimental results is 11%, which indicates high accuracy of the proposed equation.

– To help a broader application of the steel fibers in structures with the risk of a fire accident, there is a need for an efficient model to predict the tensile strength under high-temperature exposure in the design process. Using experimental results of the tensile strength at temperatures of 28 to 800 °C, and conducting regression analysis, an equation that can predict the tensile strength of plain and steel fiber reinforced concrete is proposed. The comparison of the predicted tensile strength and experimental results of N, St25, and St50 shows a deviation of 11.55%, 6.93%, and 10.96%, respectively. However, the specification of steel fiber (shape, tensile strength, and the aspect ratio of the steel fiber) can greatly effect on the tensile strength improvement and the accurately of the proposed models. Mean-

while, the heating regime including the heating rate and exposure times are other factor which can affect the results of this study. Further research on these parameter is warranted and would help researcher for a deep understand about the real behavior of the steel fiber reinforced concrete espouse to high temperature. However, the specification of steel fiber (shape, tensile strength, and the aspect ratio of the steel fiber) can affect the rate of improvement and the accuracy of the proposed models. Meanwhile, the heating regime including, the heating rate and the duration of exposure comprise other factors that can affect the results of this study. Further research on these parameters would help researchers for a deep understanding of the real behavior of the steel fiber reinforced concrete espouse to high temperature.

Declarations

Author details
[1]Present Address: Department of Civil Engineering, Faculty of Engineering, Pars University, Tehran, Iran. [2]Present Address: Department of Civil Engineering, Imam Khomeini International University, Qazvin, Iran.

References
A. C192/C192M (2012). Standard practice for making and curing concrete test specimens in the laboratory.

A.C. 363 (1984). State-of-the-art Report on High-strength Concrete (ACI 363R-84), in: American Concrete Institute.

A. Guide, A. Manual, ACI 318, Building Code Requirements for Structural Concrete (ACI 318–05) and Commentary (ACI 318R-05), ACI Committee 318, American Concrete Institute, Farmington Hills, MI, 2005 ACI 530, Building Code Requirements for Masonry Structures (ACI 530–05/ASCE 5, (n.d.).

Abaeian, R., Behbahani, H. P., & Moslem, S. J. (2018). *Effects of high temperatures on mechanical behavior of high strength concrete reinforced with high performance synthetic macro polypropylene (HPP) Fibres*. Elsevier Limited.

Abbass, W., Khan, M. I., & Mourad, S. (2018). Evaluation of mechanical properties of steel fiber reinforced concrete with different strengths of concrete. *Construction and Building Materials, 168*, 556–569.

Abdallah, S., Fan, M., & Cashell, K. A. (2017). Bond-slip behaviour of steel fibres in concrete after exposure to elevated temperatures. *Construction and Building Materials, 140*, 542–551.

Abdelrahim, M. A. A., Elthakeb, A., Mohamed, U., & Noaman, M. T. (2021). Effect of steel fibers and temperature on the mechanical properties of reactive powder concrete. *Civil and Environmental Engineering Reports., 17*, 270–276.

Ahmad, S. H., & Shah, S. P. (1985). Structural properties of high strength concrete and its implications for precast prestressed concrete. *PCI Journal, 30*, 92–119.

Ahmad, S., Umar, A., Masood, A., & Nayeem, M. (2019). Performance of self-compacting concrete at room and after elevated temperature incorporating Silica fume. *Advances in Concrete Construction., 7*, 31.

Ali, B., Kurda, R., Herki, B., Alyousef, R., Mustafa, A., Mohammed, A., Raza, A., Ahmed, H., & Fayyaz Ul-Haq, M. (2020). Effect of varying steel fiber content on strength and permeability characteristics of high strength concrete with micro silica. *Materials (basel)., 13*, 5739.

Bamonte, P., & Gambarova, P. G. (2012). A study on the mechanical properties of self-compacting concrete at high temperature and after cooling. *Materials and Structures, 45*, 1375–1387.

Bani-Yasin, I. S. (2004). *Performance of high strength fibrous concrete slab concrete connections under gravity and lateral loads*. Jordan University of Science.

Bastami, M., Baghbadrani, M., & Aslani, F. (2014). Performance of nano-Silica modified high strength concrete at elevated temperatures. *Construction and Building Materials, 68*, 402–408.

Bažant, Z. P., & Chern, J.-C. (1987). Stress-induced thermal and shrinkage strains in concrete. *Journal of Engineering Mechanics, 113*, 1493–1511.

Bošnjak, J., Sharma, A., & Grauf, K. (2019). Mechanical properties of concrete with steel and polypropylene fibres at elevated temperatures. *Fibers., 7*, 9.

C. ASTM, 496/C 496M-04, Stand. Test Method Split. Tensile Strength Cylind. Concr. Specimens. (2004).

Castillo, C. (1897). Effect of transient high temperature on high-strength concrete. (Doctoral dissertation, RiceUniversity).

Chang, Y.-F., Chen, Y.-H., Sheu, M.-S., & Yao, G. C. (2006). Residual stress–strain relationship for concrete after exposure to high temperatures. *Cement and Concrete Research, 36*, 1999–2005.

Choi, Y., & Yuan, R. L. (2005). Experimental relationship between splitting tensile strength and compressive strength of GFRC and PFRC. *Cement and Concrete Research, 35*, 1587–1591.

Craig, R. J., Parr, J. A., Germain, E., Mosquera, V., & Kamilares, S. (1986). Fiber reinforced beams in torsion. *Journal Proceedings., 83*, 934–942.

Dattatreya, J. K., & Suresh, S. (2015). Study on compressive behavior of steel fiber reinforced concrete. *Journal of Civil Engineering and Environmental Technology., 2*, 37–40.

E.C. for S. (CEN) (2004). Design of concrete structures—part 1–2: General rules—structural fire design, EN 1992 Eurocode 2.

El-Niema, E. I. (1991). Reinforced concrete beams with steel fibers under shear. *Structural Journal, 88*, 178–183.

El-Sayad, H. I. (2005). Effect of steel fibers on the compressive and splitting tensile strength of normal, medium and high strength concrete. In: Eleventh international colloquium on structural and geotechnical engineering.

Faiyadh, F. I., & Al-Ausi, M. A. (1989). Effect of elevated temperature on splitting tensile strength of fibre concrete. *International Journal of Cement Composites and Lightweight Concrete, 11*, 175–178.

Farzadnia, N., Ali, A. A. A., & Demirboga, R. (2013). Characterization of high strength mortars with nano alumina at elevated temperatures. *Cement and Concrete Research, 54*, 43–54.

Gao, D., Yan, D., & Li, X. (2012). Splitting strength of GGBFS concrete incorporating with steel fiber and polypropylene fiber after exposure to elevated temperatures. *Fire Safety Journal, 54*, 67–73.

Gündüz, Y., Taşkan, E., & Şahin, Y. (2016). Using hooked-end fibres on high performance steel fibre reinforced concrete. *High Perform. Optim. Des. Struct. Mater., II*(166), 265.

Hueste, M. B. D., Chompreda, P., Trejo, D., Cline, D. B. H., & Keating, P. B. (2004). Mechanical properties of high-strength concrete for prestressed members. *Structural Journal., 101*, 457–465.

Izadifard, R. A., Khalighi, A., Moghadam, M. A., & Pirnaeimi, H. B. (2021b). A Thoroughgoing study on engineering properties of high strength concrete at elevated temperatures. *Fire Technology.* https://doi.org/10.1007/s10694-021-01093-2

Izadifard, R. A., Abdi Moghadam, M., & Sepahi, M. M. (2021a). Influence of metakaolin as a partial replacement of cement on characteristics of concrete exposed to high temperatures. *Journal of Sustainable Cement Based Materials.* https://doi.org/10.1080/21650373.2021.1877206

Jackiewicz-Rek, W., Drzymała, T., Kuś, A., & Tomaszewski, M. (2016). Durability of high performance concrete (HPC) subject to fire temperature impact. *Archives of Civil Engineering, 62*, 73–94.

Khalil, L. W. I. (2018). Influence of high temperature on steel fiber reinforced concrete. *Journal of Engineering and Sustainable Development., 10*, 139–150.

Khaliq, W., & Waheed, F. (2017). Mechanical response and spalling sensitivity of air entrained high-strength concrete at elevated temperatures. *Construction and Building Materials, 150*, 747–757.

Kim, J., & Lee, G.-P. (2015). Evaluation of mechanical properties of steel-fibre-reinforced concrete exposed to high temperatures by double-punch test. *Construction and Building Materials, 79*, 182–191.

Kowalski, R. (2010). Mechanical properties of concrete subjected to high temperature. *Architecture Civil Engineering Environment, 2*(5), 61–70.

Kwak, Y.-K., Eberhard, M. O., Kim, W.-S., & Kim, J. (2002). Shear strength of steel fiber-reinforced concrete beams without stirrups. *ACI Structural Journal, 99*, 530–538.

Li, W., & Guo, Z. H. (1993). Experimental investigation on strength and deformation of concrete under high temperature. *Chin J Build Struct., 14*, 8–16.

Liu, Y., Shi, C., Zhang, Z., Li, N., & Shi, D. (2020). Mechanical and fracture properties of ultra-high performance geopolymer concrete: Effects of steel fiber and silica fume. *Cement and Concrete Composites, 112*, 103665.

Mansur, M. A., Vinayagam, T., & Tan, K.-H. (2008). Shear transfer across a crack in reinforced high-strength concrete. *Journal of Materials in Civil Engineering, 20*, 294–302.

Marar, K., Celik, T. (2002). The Influence of FRI on the relationship between compressive and tensile strength of NSFRC and HSFRC. In: Sixth international conference on concrete technology. Amman-Jordan.

Marques, A. M., Correia, J. R., & De Brito, J. (2013). Post-fire residual mechanical properties of concrete made with recycled rubber aggregate. *Fire Safety Journal, 58*, 49–57.

Mehdipour, S., Nikbin, I. M., Dezhampanah, S., Mohebbi, R., Moghadam, H., Charkhtab, S., & Moradi, A. (2020). Mechanical properties, durability and environmental evaluation of rubberized concrete incorporating steel fiber and metakaolin at elevated temperatures. *Journal of Cleaner Production., 254*, 120126.

Moghadam, M. A., & Izadifard, R. A. (2019). Experimental investigation on the effect of silica fume and zeolite on mechanical and durability properties of concrete at high temperatures. *SN Applied Sciences*. https://doi.org/10.1007/s42452-019-0739-2

Mitchell, D., Abrishami, H. H., & Mindess, S. (1996). The effect of steel fibers and epoxy-coated reinforcement on tension stiffening and cracking of reinforced concrete. *Materials Journal, 93*, 61–68.

Moghadam, M. A., & Izadifard, R. (2019). Evaluation of shear strength of plain and steel fibrous concrete at high temperatures. *Construction and Building Materials, 215*, 207–216.

Moghadam, M. A., & Izadifard, R. A. (2020a). Effects of zeolite and silica fume substitution on the microstructure and mechanical properties of mortar at high temperatures. *Construction and Building Materials., 253*, 119206.

Moghadam, M. A., & Izadifard, R. A. (2020b). Effects of steel and glass fibers on mechanical and durability properties of concrete exposed to high temperatures. *Fire Safety Journal, 113*, 102978.

Müller, H. S., Hilsdorf, H. K. (1990). Evaluation of the time dependent behavior of concrete, CEB Com. Euro Int. Du Béton, Bull.

Mydin, M. A. O., & Wang, Y. C. (2012). Mechanical properties of foamed concrete exposed to high temperatures. *Construction and Building Materials, 26*, 638–654.

Nadiya, S. I., & Saffar, A. (2006). Mechanical properties of steel fibrous concrete. *Al Rafdain Engineering Journal., 14*, 43–57.

Narayanan, R., & Kareem-Palanjian, A. S. (1983). Steel fibre reinforced concrete beams in torsion. *International Journal of Cement Composites and Lightweight Concrete, 5*, 235–246.

Novák, J., & Kohoutková, A. (2017). Fire response of hybrid fiber reinforced concrete to high temperature. *Procedia Engineering, 172*, 784–790.

Novak, J., & Kohoutkova, A. (2018). Mechanical properties of concrete composites subject to elevated temperature. *Fire Safety Journal, 95*, 66–76.

Patel, Y., Pasha, N., & Azam, D. (2017). Effect of different types of steel fibers on strength parameters of self compacting concrete. *International Journal of Innovative Research Science Engineering and Technology., 6*, 14727–14736.

Perumal, R. (2014). Correlation of compressive strength and other engineering properties of high-performance steel fiber–reinforced concrete. *Journal of Materials in Civil Engineering, 27*, 4014114.

Ramadoss, P. (2014). Combined effect of silica fume and steel fiber on the splitting tensile strength of high-strength concrete. *International Journal of Civil Engineering., 12*, 96–103.

Rao, K. S., & Narayana, S. (2013). Comparison of performance of standard concrete and fibre reinforced standard concrete exposed to elevated temperatures. *American Journla of Engineering Research, 3*, 20–26.

Rao, B. K. (2016). A study on steel fiber reinforced normal compacting concrete. *International Journal of Engineering Research and Applications, 6*, 41–45.

Rashid, M. A., Mansur, M. A., & Paramasivam, P. (2002). Correlations between mechanical properties of high-strength concrete. *Journal of Materials in Civil Engineering, 14*, 230–238.

Rjoub, M. I., & Muhammad, T. R. (2006). Shear capacity of high strength fiber reinforced concrete beams. *Engineering Sciences, 33*, 15–26.

Salwan, S. (2016). Effect of different types of steel fiber on the split tensile strength of sfrc cylindrical specimens. Int J AdvRes Sci Eng 642–647.

Sarbini, N. N., Ibrahim, I. S., & Saim, A. A. (2013). *Enhancement on strength properties of steel fibre reinforced concretE*. Fac. Civ. Eng. Univ. Technol.

Sharma, A. K. (1986). Shear strength of steel fiber reinforced concrete beams. *Journal Proceedings., 83*(4), 624–628.

Singh, P. R., Goel, A., Thakur, S., Shah, D. N. D. (2016). An experimental approach to Investigate Effect of steel fibers on tensile and flexural strength of fly ash concrete. Int J Sci Eng Appl Sci (IJSEAS) 2(5):384-392.

Song, P. S., & Hwang, S. (2004). Mechanical properties of high-strength steel fiber-reinforced concrete. *Construction and Building Materials, 18*, 669–673.

Srikar, V. V. M., & Kalyan, G. (2018). International journal of engineering sciences & research technology performance of concrete with adding of steel fibers. *International Journal of Engineering Science Research and Technology., 7*, 290–308.

Standard, B. (2009). *Testing hardened concrete* (pp. 12390–12393). Compressive Strength Test Specimens.

Sukumar, A., & John, E. (2014). Fiber addition and its effect on concrete strength. *International Journal of Innovative Research in Advanced Engineering., 1*, 144–149.

Sumathi, A., & Saravana, K. (2014). Strength predictions of admixed high performance steel fiber concrete. *ChemTech, 6*, 4729–4736.

Thomas, J., & Ramaswamy, A. (2007). Mechanical properties of steel fiber-reinforced concrete. *Journal of Materials in Civil Engineering, 19*, 385–392.

Uysal, M., Yilmaz, K., & Ipek, M. (2012). Properties and behavior of self-compacting concrete produced with GBFS and FA additives subjected to high temperatures. *Construction and Building Materials, 28*, 321–326.

Vairagade, V. S., Kene, K. S., & Patil, T. R. (2012). Comparative study of steel fiber reinforced over control concrete. *International Journal of Scientific and Research Publications, 2*, 1–3.

Wadekar, A. P., & Pandit, P. R. D. (2014). Study of different types fibres used in high strength fibre reinforced concrete. *International Journal of Innovative Research in Advanced Engineering., 1*, 225–230.

Wafa, F. F., & Ashour, S. A. (1992). Mechanical properties of high-strength fiber reinforced concrete. *Materials Journal., 89*, 449–455.

Xiao, J., Xie, Q., & Xie, W. (2018). Study on high-performance concrete at high temperatures in China (2004–2016)-An updated overview. *Fire Safety Journal, 95*, 11–24.

Xie, D., & Qian, Z. (1998). Research on bond and tension of concrete after high temperature. *Journal of Zhejiang University Natural Sciences Edition, 32*, 597–602.

Xu, B. W., & Shi, H. S. (2009). Correlations among mechanical properties of steel fiber reinforced concrete. *Construction and Building Materials, 23*, 3468–3474.

Yan, K., Xu, H., Shen, G., & Liu, P. (2013). Prediction of splitting tensile strength from cylinder compressive strength of concrete by support vector machine. *Advances in Materials Science and Engineering, 2013*, 1–13.

Yermak, N., Pliya, P., Beaucour, A.-L., Simon, A., & Noumowé, A. (2017). Influence of steel and/or polypropylene fibres on the behaviour of concrete at high temperature: Spalling, transfer and mechanical properties. *Construction and Building Materials, 132*, 240–250.

Publisher's Note

Springer Nature remains neutral with regard to jurisdictional claims in published maps and institutional affiliations.